Inhibitory effect of morin on aldolase 2 from *Eimeria tenella*

Junjing Hu [a,b], Mingfei Sun [b], Nanshan Qi [b], Asmaa M.I. Abuzeid [a,c], Juan Li [b], Haiming Cai [b], Minna Lv [b], Xuhui Lin [b], Shenquan Liao [b,**], Guoqing Li [a,*]

[a] *Guangdong Provincial Key Laboratory of Zoonosis Prevention and Control, College of Veterinary Medicine, South China Agricultural University, Guangzhou, 510542, China*
[b] *Zhaoqing Branch Center of Guangdong Laboratory for Lingnan Modern Agricultural Science and Technology, Maoming Branch Center of Guangdong Laboratory for Lingnan Modern Agricultural Science and Technology, Key Laboratory of Livestock Disease Prevention of Guangdong Province, Scientific Observation and Experiment Station of Veterinary Drugs and Diagnostic Techniques of Guangdong Province, Ministry of Agriculture and Rural Affairs, Key Laboratory of Avian Influenza and Other Major Poultry Diseases Prevention and Control, Ministry of Agriculture and Rural Affairs, Institute of Animal Health, Guangdong Academy of Agricultural Sciences, Guangzhou, 510640, Guangdong, PR China*
[c] *Faculty of Veterinary Medicine, Suez Canal University, Ismailia, 41522, Egypt*

ARTICLE INFO

ABSTRACT

Eimeria tenella (*E. tenella*) is a protozoal parasite that can cause severe cecal lesions and death in chickens, seriously harming the chicken industry. Conventional control strategies mainly rely on anticoccidial drugs. However, the emerging problems of anticoccidial resistance and drug residues necessitate exploring potential drug targets for developing new anticoccidial drugs. Fructose-1,6-bisphosphate aldolase (ALD) is an essential enzyme for parasite energy metabolism that has been considered a potential drug target. In this study, we analyzed the molecular and biochemical properties of *E. tenella* ALD2 (*Et*ALD2). *Et*ALD2 mRNA expression was highest in second-generation merozoites, whereas the protein level was highest in unsporulated oocysts. Indirect immunofluorescence showed that *Et*ALD2 was mainly distributed in sporozoite' cytoplasm. The natural product inhibitor (morin) was screened by computer-aided drug screening. Enzyme kinetic and inhibition kinetic assays showed that morin had a good inhibitory effect on *Et*ALD2 activity (IC_{50} = 10.37 μM, Ki = 48.97 μM). *In vitro* inhibition assay demonstrated that morin had an inhibitory effect on *E. tenella* development, with an IC_{50} value of 3.98 μM and drug selection index of 177.49. *In vivo*, morin significantly improved cecal lesions ($p < 0.05$) and reduced oocyst excretion ($p < 0.05$) in *E. tenella*-infected chickens compared with the untreated group. The anticoccidial index of the group receiving 450 mg morin per kg feed was 162, showing a good anticoccidial effect. These findings suggest that *Et*ALD2 could be a novel drug target for *E. tenella* treatment, and morin should be further evaluated as a therapeutic candidate for chicken coccidiosis.

1. Introduction

Coccidiosis is one of the most critical diseases in chickens (Blake et al., 2020; El-Shall et al., 2022; Lee et al., 2022) caused by the coccidian parasites *Eimeria* species infecting the intestinal epithelial cells of chickens. *Eimeria* species have a worldwide distribution and seriously harm the chicken industry, resulting in substantial economic losses (El-Liu et al., 2020). The annual cost of coccidiosis prevention and treatment exceeds USD 14.5 billion worldwide (Blake et al., 2020). Among the seven known species (Zhang et al., 2013), *Eimeria tenella* (*E. tenella*) is the most common and clinically pathogenic species that can cause

severe cecal lesions and death in chickens (Zhang et al., 2022). Although coccidia control mainly depends on anticoccidial drugs, there are growing concerns about anticoccidial resistance and drug residues. Thus, more efforts are required to identify potential drug targets and develop new anticoccidial therapeutics for controlling coccidiosis in chickens.

During the endophytic developmental stage, the parasitic protozoa mainly live in hypoxic or anaerobic environments and thus use glycolysis as one of the primary ways to obtain energy. Fructose-1,6-bisphosphate aldolase (EC:4.1.2.13) is an essential enzyme for glycolysis. This enzyme catalyzes the reversible cleavage of fructose-1,6-

bisphosphate (FBP) to dihydroxyacetone phosphate (DHAP) and glyceraldehyde-3-phosphate (GAP) (Yang et al., 2019). Aldolase plays a central role in glycolysis, gluconeogenesis, and fructose metabolism (Bu et al., 2018; Pirovich et al., 2021). Previous studies have reported that aldolase (ALD) is essential for energy metabolism in some protozoan parasites (Dax et al., 2006; Cáceres et al., 2010; Pirovich et al., 2021). Therefore, ALD has been considered a potential antiprotozoal drug target. However, the molecular and biochemical properties of *E. tenella* aldolase 2 (*Et*ALD2) have been poorly studied.

Morin is a vital flavonoid compound in mulberry, with anti-inflammatory (Wei et al., 2015), antibacterial (Li et al., 2020), and anti-tumor effects (Gao et al., 2021). While morin has been extensively researched, there are few reports on its antiparasitic effects. Preliminary virtual screening and molecular docking suggested that morin may have high inhibitory activity on *Et*ALD2.

In this study, we investigated the molecular and biochemical properties of *Et*ALD2 in *E. tenella* for the first time. Additionally, we analyzed the inhibitory effects of the natural product morin on *Et*ALD2 enzymatic activity. Our results suggest *Et*ALD2 as a potential drug target against *E. tenella,* and morin may be a promising anticoccidial drug candidate for chicken coccidiosis.

2. Materials and methods

2.1. Animals and parasites

Chickens used in this study were bred by the Institute of Animal Science, Guangdong Academy of Agricultural Sciences (GAAS) and then transported to the experimental animal house of the Institute of Animal Health, GAAS. The Guangdong strain of *E. tenella* was isolated and preserved by the Laboratory of Parasitic Biology, Institute of Animal Health, GAAS, with propagation every four months. Unsporulated oocysts (UO) were isolated from the cecal content of *E. tenella*-infected chickens seven days post-infection (pi). The unsporulated oocysts were incubated in 2.5% potassium dichromate at 28 °C in a water bath shaking bed to collect sporulated oocysts (SO). The sporozoites (Spz) were collected and purified from SO during *in vitro* excystation (Han et al., 2010; Liang et al., 2021). Second-generation merozoites (Mrz) were isolated from the ceca of infected chickens 115 h post-infection, according to Zhou et al. (2010). Samples from all development stages were stored in liquid nitrogen.

2.2. EtALD2 sequence analysis

The *Et*ALD2 gene was identified from the *E. tenella* genome (GenBank accession number: GCA_000499545.1) annotated as "TIM Superfamily" (BioProjects: PRJEB4863) (Cai et al., 2003). To identify *Et*ALD2 homologous genes in Apicomplexa, the genome data of six representative species, *Eimeria tenella, Babesia bovis, Cyclospora cayetanensis, Neospora caninum, Plasmodium falciparum,* and *Toxoplasma gondii,* were downloaded from NCBI (https://www.ncbi.nlm.nih.gov/). Multiple sequence alignment of the gene sequences homologous to *Et*ALD2 was performed by ClustalW (Edgar and Sjolander, 2004). A rooted phylogenetic tree was constructed using MEGA7 (Kumar et al., 2016), where the neighbor-joining (NJ) method with the Jones–Taylor–Thornton (JTT) model was used based on 1000 bootstrap replicates.

2.3. Total RNA extraction and first-strand cDNA synthesis

Total RNA was extracted from *E. tenella* at four different developmental stages (sporozoites, second-generation merozoites, unsporulated oocysts, and sporulated oocysts) by the MicroElute Total RNA Kit (Omega Bio-tek, Guangzhou, China). Briefly, samples were lysed with TRK lysis buffer, then added to a MicroElute® RNA Mini Column, centrifuged, and washed with RWF Wash Buffer. DNase buffer was used to digest the retained genomic DNA in the RNA Mini Column, and the

column was washed with RNA Wash Buffer. A 20 μL DEPC water was added to elute the RNA. RNA quality was tested using a spectrophotometer ($OD_{260}/OD_{280} \approx 2.0$), while RNA integrity was assessed by agarose gel electrophoresis. The first-strand cDNA was synthesized using the PrimeScript RT Reagent Kit (TaKaRa, Guangzhou, China) and stored at −20 °C.

2.4. Cloning of the EtALD2 gene

Primers were designed to amplify the *Et*ALD2 coding region based on the *Et*ALD2 sequence in GenBank (Gene ID: XP_013233987.1). The primer sequences were *Et*ALD2-F: 5′-CGCGGATCCTTC-GATTCTTTTGGGGTTTCGT-3′ and *Et*ALD2-R: 5′-CGCAAGCTTC-CAAGGCGAGGTAGCAAACC-3'. The underlined parts represent *Bam*HI and *Hind* III restriction sites, respectively. Pooled cDNA sample of the four developmental stages of *E. tenella* was used as a template. PCR reaction (50 μL) contained cDNA (1 μL), forward and reverse primers (10 pmol/L, 1 μL of each), 2 × E-Taq DNA (25 μL, TaKaRa, Guangzhou, China), and ddH₂O (22 μL). The PCR conditions were as follows: pre-denaturation at 94 °C for 5 min; 35 cycles of denaturation at 94 °C for 30 s, annealing at 57 °C for 30 s, and extension at 72 °C for 90 s; and final extension at 72 °C for 7 min. PCR products were identified by 1% agarose gel electrophoresis and purified using the TIAN gel Midi Purification Kit (Tiangen, Beijing, China) following the manufacturer's protocol. The recovered PCR products were ligated into the pColdI vector (laboratory preservation) following digestion with *Bam*HI and *Hind* III. The ligation mixture was transformed into BL21 (DE3) competent *E. coli* cells (Vazyme, Nanjing, China) and spread on Luria-Bertani (LB) agar plates supplemented with kanamycin. A single white colony was mixed into LB broth/0.1% kanamycin and incubated (160 rpm, 37 °C, 8 h). The positive plasmid was screened by double-enzyme digestion, purified by TIANprep Mini Plasmid Kit (Tiangen, Beijing, China), and sent to Sangon Biotech (Shanghai, China) for sequencing. The correctly sequenced plasmid was named pColdI-*Et*ALD2.

2.5. EtALD2 expression and identification

The expression of the recombinant pColdI-*Et*ALD2 protein was performed in BL21 *E. coli* cells (Vazyme, Nanjing, China). The pColdI-*Et*ALD2 strain was cultured in Luria-Bertani (LB) broth with 0.1% kanamycin at 37 °C with shaking at 160 rpm until the optical density OD_{600} value reached 0.6. Isopropyl *β*-d-1-thiogalactopyranoside (IPTG, 0.1 mmol/L) was added to induce expression overnight at 16 °C. After centrifugation (5000×*g*, 5 min), the supernatant and precipitate were collected for SDS-PAGE (sodium dodecyl sulfate-polyacrylamide gel electrophoresis) to analyze protein expression. The recombinant bacterial solution (100 mL) with induced expression was ultrasonically lysed on ice by the JY92-2D ultrasonic cell crusher (Xinzhi, Ningbo, China) at 200 W for 10 min, with an interruption for 2 s every 2 s of sonication. The supernatant was collected by centrifugation (10,000×*g*, 20 min) and transferred to a nickel column containing gel included in the His-tag Protein Purification Kit (Beyotime, Shanghai, China). After thorough loading, the column was incubated at 4 °C for 1 h. The protein was purified following the instructions of the His-tag Protein Purification Kit, and protein concentration was determined using the Bradford Protein Concentration Assay Kit (Beyotime, Shanghai, China).

Purified *Et*ALD2 proteins were subjected to 12% SDS-PAGE and electro-transferred to nitrocellulose membranes (Pall co., Port Washington, NY, USA). The membranes were placed in Phosphate-Buffered Saline-Tween (PBST) with 5% (w/v) skimmed milk powder for blocking for 1 h at 37 °C. For Western blot analysis, blocked membranes were incubated overnight at 4 °C with mouse anti-*Et*ALD2 antibodies (1:2000) (prepared by GenScript Company, Nanjing, China), positive serum from chickens infected with *E. tenella* (1:500), and healthy chicken serum (1:500) as primary antibodies. After washing in PBST, membranes were incubated with the corresponding secondary

antibodies, goat anti-mouse IgG-HRP (Horseradish Peroxidase-conjugated) antibodies (1:2000, CWBIO, Beijing, China) and rabbit anti-chicken IgG-HRP antibodies (1:2000, Cell Signaling Technology, Shanghai, China) for 1 h at 37 °C. After washing with PBST, immuno-reactive bands were visualized using the diaminobenzidine (DAB) Western blotting detection system (Beyotime, Shanghai, China) for enhanced chemiluminescence (ECL).

2.6. Transcriptional level analysis of EtALD2

Quantitative reverse transcription PCR (qRT-PCR) was used to analyze the differential transcriptional level of *Et*ALD2 using cDNA isolated from *E. tenella* at the four developmental stages as a template. *Et*18srRNA was selected as the reference gene and *Et*ALD2 gene as the target gene. Primers for qRT-PCR were designed to analyze the differences in *Et*ALD2 mRNA expression at the four developmental stages of *E. tenella*. The primer sequences for the target gene were *qEt*ALD-F: 5′-TCGATTGGGGTGGAGAACAC-3′ and *qEt*ALD-R: 5′-TATCCCCGGAAT-GATCCCCT. The primers for the reference gene were 18srRNA-F: 5′-TGTAGTGGAGTCTTGGTGATTC-3′ and 18srRNA-R: 5′-CCTGCTGCCTTCCTTAGATG-3'. qPCR reactions (10 μL) contained cDNA (1 μL), forward and reverse primers (10 μmol/L, 0.8 μL of each), TB Green Premix Ex TaqII (5 μL, TaKaRa, Guangzhou, China), and ddH$_2$O (2 μL). qPCR cycling program was 95 °C for 30 s; 35 cycles of 95 °C for 15 s, 60 °C for 30 s; 95 °C for 10s; and melt curve stage at 65–95 °C, increasing 0.5 °C every 5 s. Each sample was examined in triplicates. The relative expression levels of *Et*ALD2 in the different developmental stages were calculated by the $2^{-\Delta\Delta CT}$ method.

2.7. Translation level analysis of EtALD2

The *Et*ALD2 protein levels were analyzed by Western blot. Samples (0.2 g) of *E. tenella* four developmental stages (UO, SO, Spz, and Mrz) were placed into 1.5 mL centrifuge tubes. After adding 300 μL radio-immunoprecipitation assay (RIPA) buffer (Beyotime, Shanghai, China) and 3 μL protease inhibitor (Sigma-Aldrich, Guangzhou, China), centrifuge tubes were oscillated at 60 HZ for 40 min to extract total proteins. The total proteins were separately extracted from the four developmental stages, and the protein concentration was determined using the Bradford Protein Concentration Assay Kit. Based on the measured protein concentrations, the amount of protein loaded in SDS-PAGE from the four stages was adjusted to keep final concentrations consistent. Western blot was performed using mouse anti-*Et*ACTIN monoclonal antibodies and mouse polyclonal antibodies against *Et*ALD2 (prepared by GenScript Company, Nanjing, China) as primary antibodies. *Et*ACTIN was used as a reference. The secondary antibody was goat anti-mouse IgG-HRP (1:2000, CWBIO, Beijing, China). The results were analyzed using ImageJ software.

2.8. Indirect immunofluorescence of EtALD2 localization in sporozoites

We determined the localization of *Et*ALD2 protein in sporozoites by indirect immunofluorescence assay (IFA). The sporozoites were fixed on slides with 4% paraformaldehyde for 30 min, permeated with 1% Triton® X-100 for 25 min, and blocked with 10% bovine serum albumin (BSA, Sangon Biotech, Shanghai, China) for 1 h. The slides were then incubated with mouse anti-r*Et*ALD2 polyclonal antibodies (1:300) and mouse pre-immune serum as a negative control (1:100) overnight at 4 °C and with AlexaFluor™ 488 rabbit anti-mouse-IgG-R (1:500, Cell Signaling Technology, Shanghai, China) for 1 h at 37 °C in the dark. Nuclei were stained with 10 μg/mL of 4′,6-diamidino-2-phenylindole (DAPI, Sigma-Aldrich) for 10 min at room temperature. After three washes with phosphate buffer saline (PBS), the sporozoites were examined for fluorescent staining under a Zeiss LSM710 confocal microscope (Zeiss Microscopy, White Plains, NY, USA).

2.9. Analysis of EtALD2 enzyme kinetics and inhibition

We evaluated the catalytic activity of r*Et*ALD2 on fructose 1,6-bisphosphate (FBP or F16BP) cleavage by measuring the NADH consumption rate using the change in relative fluorescence units (ΔRFU), measured by Varioskan™ LUX with an excitation wavelength of 340 nm and an emission wavelength of 460 nm. Reactions were conducted for 30 min at 27.5 °C in 50 mM Tris-HCl buffer (pH 7.5, 100 μL total volume). The reaction system contained 75 ng r*Et*ALD2, 0.3 mM NADH (Sigma-Aldrich), 0.2 mg/mL BSA, 0.2 U/mL triosephosphate isomerase (TPI, Sigma-Aldrich), 2.25 U/mL α-glycerophosphate dehydrogenase (GDH, Sigma-Aldrich), and 0.1 mM FBP (Sangon Biotech). *Et*ALD2 enzyme kinetic Michaelis-Menten curves were determined using different substrate concentrations, including NADH (3.125, 6.25, 12.5, 25, 50, and 100 μM) and FBP (25, 50, 75, 100, 200, and 300 μM). One unit (U) of *Et*ALD2 activity represented the amount of enzyme that catalyzes the cleavage of fructose-1,6-bisphosphate to α-glycerol phosphate (glycerol-3-phosphate) and produces 1.0 mol/L of NAD$^+$ per minute at 27.5 °C. Dimethyl sulfoxide (DMSO, Sigma-Aldrich) was used to dissolve morin (Yuanye, Shanghai, China) at a storage concentration of 12.5 mM. The inhibition constant (*Ki*) of morin on *Et*ALD2 was determined. The reaction system (100 μL) contained 75 ng r*Et*ALD2, 0.2 mg/mL BSA, 0.2 U/mL TPI, 2.25 U/mL GDH, 1 mM FBP/0.5 mM NADH, different concentrations of NADH/FBP, and 25 μM morin. All experiments were performed using 75 ng of r*Et*ALD2 and repeated three times. Kinetic data were plotted using GraphPad Prism software. The initial rate (RFU/min) was determined based on Michaelis-Menten enzyme kinetics, and *Km*, *Vmax*, *Kcat*, *Ki*, and IC$_{50}$ values of the substrate were calculated.

2.10. MTT cytotoxicity assay

Referring to Jin et al. (2019), Madin-Darby bovine kidney cells (MDBK, Jennio, Guangzhou, China) grown to 80% confluency were digested with 0.25% trypsin digestion solution (BioFroxx, Guangzhou, China). Cells were seeded in a 24-well culture plate (1 × 10^4 cells/well) and incubated in a cell culture incubator (5% CO$_2$, 37 °C, 24 h). When the cells in the culture plate grew to 80% confluency or above, morin was added at 31.25, 62.5, 125, 250, 500, and 1000 μM. Blank control and three replicates of each group were set, with continuing incubation at 5% CO$_2$/37 °C. After 48 h incubation, 10 μL MTT (2,5-diphenyl-2H-tetrazolium bromide) reagent (5 mg/mL, Roche, Beijing, China) was added to each well and then cultured in the cell culture incubator for 4 h. A 100 μL MTT solution was added to dissolve Metzan crystal in each well, followed by shaking on a rotating shaker for 10 min. A multifunctional microplate reader was used to measure the absorbance at 550 nm. The OD$_{550}$ values of the experimental and the blank control groups were determined to judge the cell viability and the toxicity of the inhibitors on the cells. Data were processed using GraphPad Prism7 software, and CC$_{50}$ values (half cytotoxicity concentration) were calculated. All cytotoxicity tests were repeated three times.

Relative cell viability (%) = OD$_{550}$ value of drug group/ OD$_{550}$ value of blank control group × 100%

2.11. Inhibitory effect of morin on E. tenella in vitro

In vitro inhibition of *E. tenella* by morin was studied according to Marugan-Hernandez et al. (2020), Thabet et al. (2017), and Sun et al. (2016). MDBK cells were digested with 0.25% trypsin when they reached 80% confluency. Then, 2 × 10^5 cells were seeded in 24-well plates with Minimum Essential Medium (Gibco™, Thermo Fisher Scientific, Guangzhou, China) with 10% fetal bovine serum (FBS) and incubated at 37 °C, 5% CO$_2$ for 24 h. When the cells reached 80%

confluency, 5×10^4 *E. tenella* sporozoites were inoculated per well, and the medium was discarded after 4 h. The MDBK/sporozoites suspensions were washed three times with PBS, followed by centrifugation to discard the supernatant, and MEM with 5% FBS was added to each well. Morin was added at final concentrations of 0.01, 0.1, 1, and 10 μM, with three replicates per experimental condition. Meanwhile, a blank control (MDBK cells without sporozoites and inhibitors) and positive control (MDBK cells with sporozoites and without inhibitors) were prepared. Then, 10 μM sulfachlorpyrazine sodium (SS) was used as a positive drug control with MDBK cells and sporozoites. The prepared plate was incubated in 5% CO_2 at 37 °C for 48 h before discarding the medium. Cells in each well were washed three times with PBS before being used to extract total RNA by the MicroElute Total RNA Kit (Omega Bio-tek). qRT-PCR was used to detect the effect of morin on the development of *E. tenella* using the One-Step TB Green® PrimeScript™ RT-PCR Kit II (TaKaRa). Primers used were *Et*GAPDH-F: 5′-TGGAGTCTTCACGAAC AAGGA-3′, *Et*GAPDH-R: 5′-ACCCATCACAAACATCGGAGTA-3′, BGAPD H-F: 5′-GAAGGTCGGAGTGAACGGAT-3′, and BGAPDH-R: 5′-GAAGGT CGGAGTGAACGGAT-3′. *Et*GAPDH and BGAPDH primers were used to assess the mRNA expression of *E. tenella* GAPDH (target gene) and MDBK cells GAPDH (internal reference gene), respectively. qRT-PCR reactions (20 μL) contained RNA (1 μL), forward and reverse primers (1 μmol/L), 2 × One-Step TB Green RT-PCR Buffer (10 μL), PrimeScript 1 Step Enzyme Mix (1 μL), and RNase Free ddH$_2$O (6 μL). qRT-PCR conditions were 42 °C for 5 min; 95 °C for 30 s; 95 °C for 5 s, 60 °C for 20 s, 40 cycles; 95 °C for 10 s; and Melting curve at 65–95 °C, increasing 0.5 °C every 5 s. The following formula was used to calculate the inhibitory effect of morin on *E. tenella*.

$$\text{Inhibition} \ (\%) = 100 \times (1 - 2^{-\triangle\triangle\text{CT}})$$

According to Jin et al. (2019), safety interval (SI) was calculated by measuring the ratio of CC_{50} to IC_{50} (half effective concentration), that is, $SI = CC_{50}/IC_{50}$. Theoretically, the index >1 indicates that the drug is effective and safe, and the higher the SI value is, the safer the drug will be.

2.12. Evaluation of anticoccidial effect of morin in vivo

Forty 12-day-old healthy Lingnan yellow chickens of similar size and body shape were randomly selected and divided into four groups. Each group was weighed (denoted as the initial weight before infection), and the weight was adjusted appropriately to keep the weight of each group consistent. Chickens receiving morin at 150 and 450 mg/kg feed doses were classified as Group1 (G1 group) and Group2 (G2 group), respectively. The infected group was designated as the positive control group (PC group), while the non-infected group was designated as the blank control group (NC group). The G1 and G2 groups were given feed containing the corresponding concentration of morin two days before the coccidial challenge. PC and NC groups were given a basal diet. After two days, chickens in all groups, except the NC group, were fed on 1×10^4 *E. tenella* sporulated oocysts. The anticoccidial efficacy of morin was evaluated *in vivo* according to the anticoccidial index (ACI) by referring to Qaid et al. (2021). The ACI≥180 was considered excellent, $160 \leq$ ACI<180 was judged good, $120 \leq$ ACI<160 was medium, and ACI<120 was invalid.

2.13. Statistical analysis

Statistical analysis was performed using IBM SPSS Statistics 26. One-way analysis of variance with Duncan's multiple range test was used to compare groups, and *p*-values of less than 0.05 were considered statistically significant.

3. Results

3.1. Analysis of EtALD2 sequence

Analysis of the conserved structure of *Et*ALD2 revealed that the *Et*ALD2 protein was composed of 368 amino acids and contained a PTZ00019 conserved domain, which belongs to the TIM superfamily (Fig. 1A). Analyzing *Et*ALD2 homologs from different parasite species showed that the sequences of the *Et*ALD2 domain shared a high degree of similarity with the ALD domain from apicomplexan parasites. Furthermore, the *Et*ALD2 gene contained a class I aldolase motif (Fig. 1B). In the phylogenetic tree, *Et*ALD2 was closely related to ALDs from other apicomplexan species, *Cyclospora cayetanensis* (OEH7 8062.1), *Toxoplasma gondii* (4D2J_A, BN1205_061240), and *Neospora caninum* (NCLIV_050370). *Et*ALD2 clustered in one branch with ALD from *C. cayetanensis* (OEH78062.1). However, ALD from *Toxoplasma gondii* and *Neospora caninum* clustered together (Fig. 1C).

3.2. Purification and immunogenicity analysis of recombinant EtALD2 protein

SDS-PAGE analysis of the bacterial culture media before and after induction, using supernatants and precipitates after bacterial lysis, demonstrated that the target protein was partially expressed in the supernatant with visible bands at approximately 40 kDa (Fig. 2A). We successfully obtained pCold I-*Et*ALD2 soluble protein using the Beyotime His-tag Protein Purification Kit (Fig. 2B). Western blot results showed that the protein could be specifically recognized by anti-*Et*ALD2 polyclonal antibodies and *E. tenella*-infected chickens' positive serum. However, no reaction band was found with uninfected chicken serum (Fig. 2C).

3.3. Subcellular EtALD2 localization in sporozoites

Laser scanning was performed with a Zeiss LSM710 confocal microscope at an excitation light wavelength of 493 nm with an emission wavelength of 519 nm (*Et*ALD2) and an excitation light wavelength of 405 nm with an emission wavelength of 498 nm (DAPI). In Fig. 3, blue fluorescence represents the DAPI-labeled nucleus, and red fluorescence shows the *Et*ALD2 signal. *Et*ALD2 proteins were evenly distributed in the cytoplasm of sporozoites.

3.4. Analysis of EtALD2 transcription and translation levels

*Et*ALD2 mRNA expression levels significantly differed ($p < 0.05$) between the four developmental stages of *E. tenella*. Second-generation merozoites expressed the highest level of *Et*ALD2 mRNA, followed by sporulated oocysts, sporozoites, and unsporulated oocysts (Fig. 4A). *Et*ALD2 protein expression was also measured in the different developmental stages of *E. tenella*, using *Et*ACTIN as an internal reference. As shown in Fig. 4B and C, *Et*ALD2 protein expression varied significantly among the four stages. The highest protein level was detected in unsporulated oocysts, followed by sporulated oocysts, second-generation merozoites, and sporozoites ($p < 0.05$).

3.5. EtALD2 activity and inhibition by morin

*Et*ALD2 had catalytic activity on fructose 1, 6-diphosphate (Fig. 5A). According to response surface methodology (RSM), the optimal reaction conditions for *Et*ALD2 enzyme activity were 27.5 °C and pH 7.5 (Fig. 5B). We assessed *Et*ALD2 enzyme activity by enzyme kinetic experiment. The nonlinear Michaelis-Menten equation was fitted by Enzyme Kinetics Module GraphPad Prism 7 to obtain the kinetic parameters *Km, Vmax,* and *Kcat* (Fig. 5C and D and Table 1). For FBP, *Km* $= 18.06 \pm 1.40$ μM and *Vmax* $= 0.64 \pm 0.01$ mmol/min/mg; and for NADH, *Km* $= 43.84 \pm 6.59$ μM and *Vmax* $= 2.04 \pm 0.17$ mmol/min/mg.
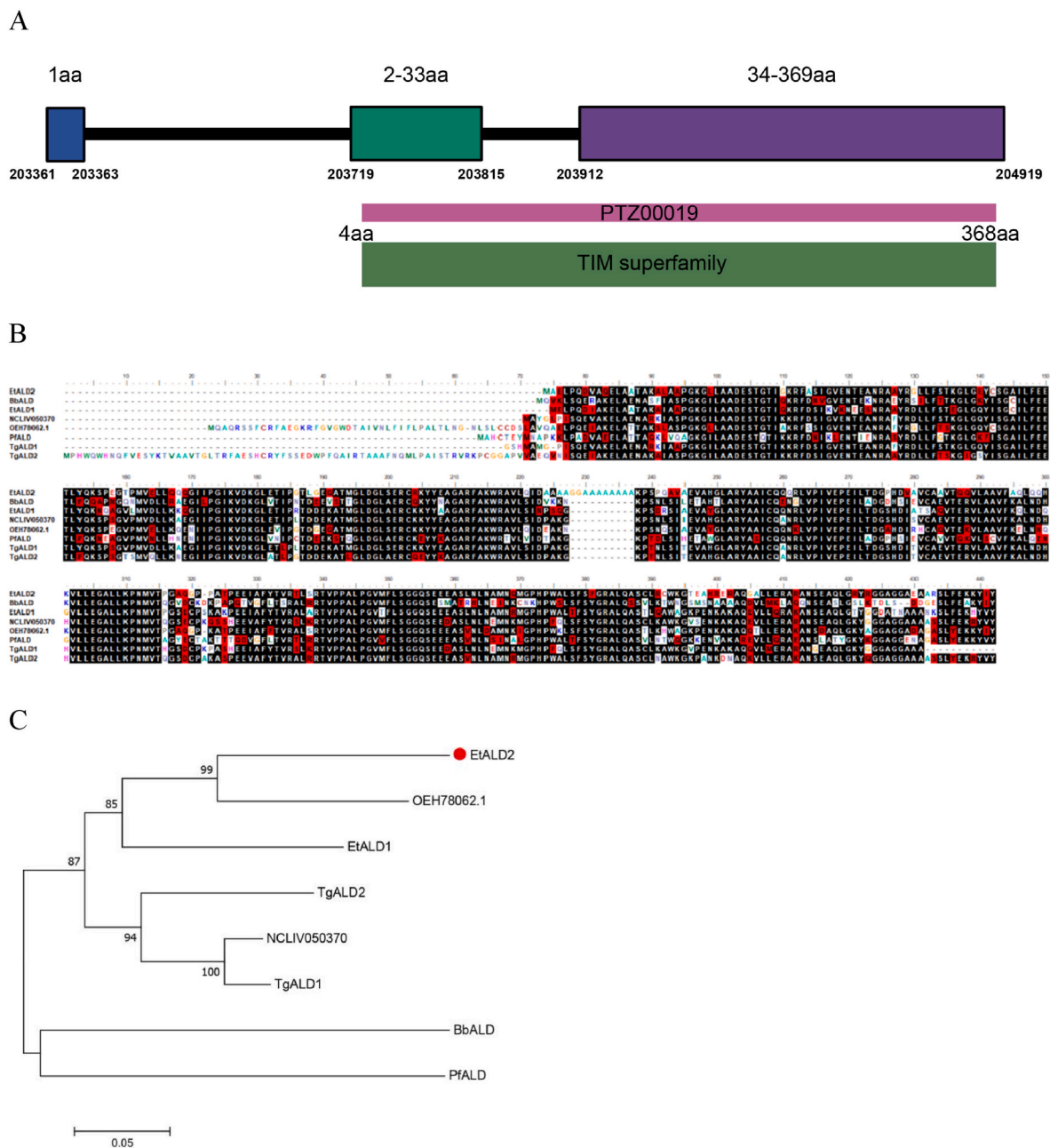
Fig. 1. Conserved domain, multiple sequence alignment and evolutionary analysis of *Et*ALD2 sequence. A. *Et*ALD2 conserved domain analysis. B. Multiple sequence alignment of *Et*ALD2 homologs from different species. C. Phylogenetic analysis of *Et*ALD2 and homologs from other apicomplexans inferred by neighbor-joining method.

In the *Et*ALD2 catalytic activity inhibition experiment, morin could inhibit the catalytic activity of *Et*ALD2. Fig. 5E and F shows the enzyme kinetic inhibition curve of morin. The *Ki* value and IC$_{50}$ value of morin were 48.97 μM and 10.37 μM, respectively.

3.6. Cytotoxicity of morin on MDBK cells

We used the MTT method to evaluate the cytotoxicity of morin on MDBK cells. Results revealed that the CC$_{50}$ value of morin on MDBK cells was 706.4 μM, and MDBK cells had no toxicity at 250 μM morin and below (Fig. 6A). The negative control well supplemented with 0.5% DMSO showed no toxicity effect on MDBK cells.

3.7. Inhibition of E. tenella by morin in vitro

The effect of morin on *E. tenella* was tested *in vitro*. As a positive control, 10 μM sulfachlorpyrazine sodium (SS) inhibited parasite growth by 74.32% at the endogenous developmental stage (sporozoites) (Fig. 6B). Compared with the positive control, morin showed anti-*E. tenella* activity on the endogenous developmental stage, with a drug concentration in the micromolar range. A significant difference (*p* < 0.05) was identified in the inhibition rate between the morin-added and the positive control groups. The IC$_{50}$ value for *E. tenella* inhibition at the endogenous stage was 3.98 μM (Fig. 6B).

3.8. Cecal lesion scores

On the seventh day after the coccidial attack, chickens in each group
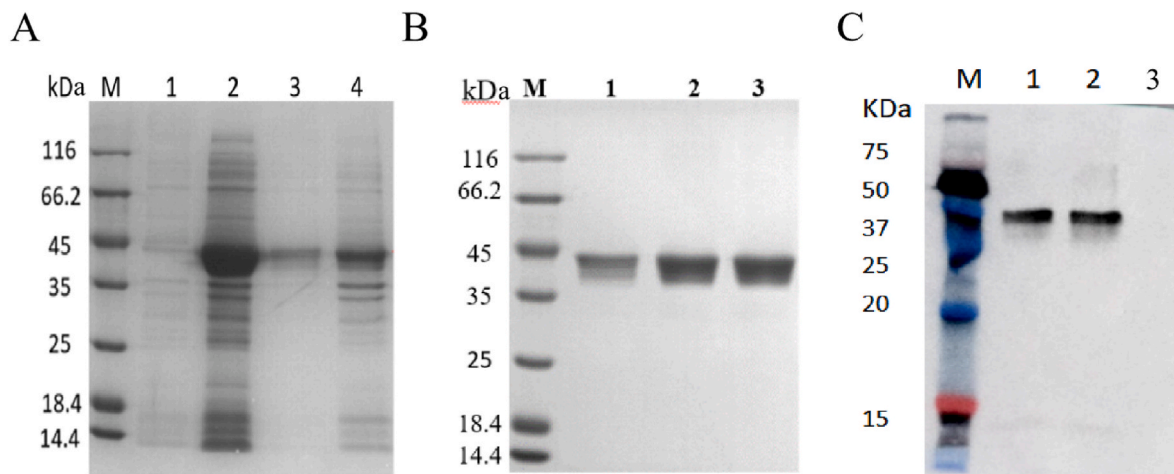
Fig. 2. SDS-PAGE and Western blot analysis of recombinant pCold I-*Et*ALD2. M: Protein marker; A. 1: Bacterial culture media before induction; 2: Bacterial culture media after induction; 3: Supernatants after bacterial lysis; 4: Precipitates after bacterial lysis; B. 1–3: Purified pCold I-*Et*ALD2 protein; C. 1 : Recombinant proteins detected by anti-*Et*ALD2 polyclonal antibody; 2 : Recombinant proteins detected by serum of infected chicken; 3 : Recombinant proteins detected by serum of healthy chicken.
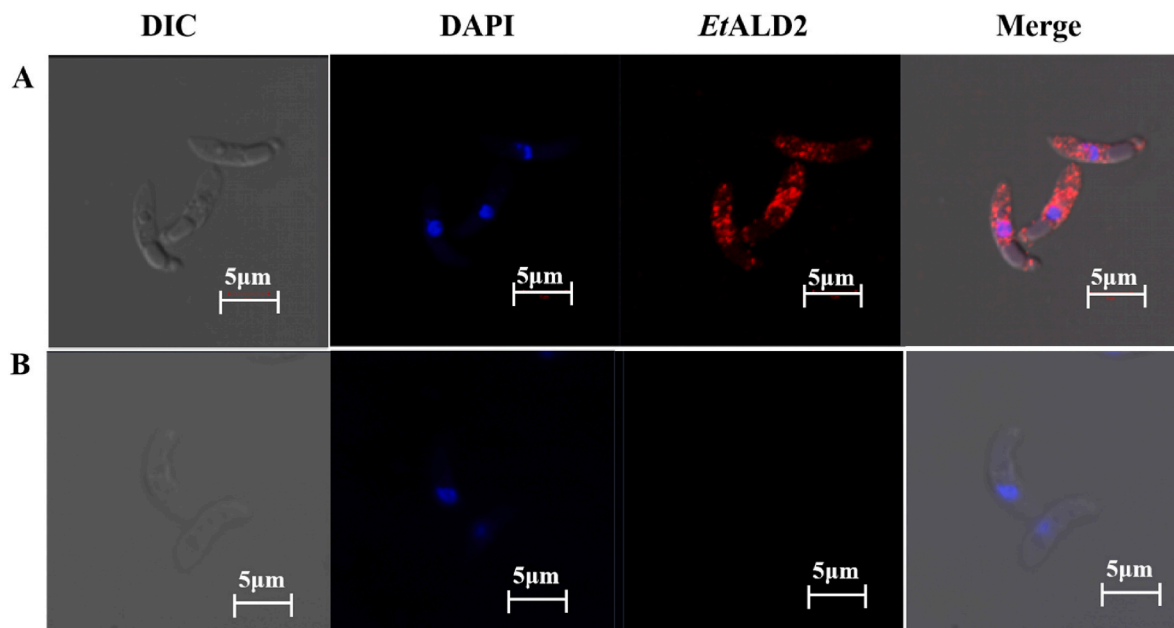

Fig. 3. *Et*ALD2 localization in *E. tenella* sporozoites incubated with mouse anti-*Et*ALD2 antibody (A) and pre-immunization mouse serum (B). DIC: Images of sporozoites under visible light; DAPI: Images observed at an excitation light wavelength of 405 nm and emission wavelength of 498 nm; *Et*ALD2: Images observed at an excitation light wavelength of 493 nm and emission wavelength of 519 nm; Merge: Images of sporozoites observed by laser confocal microscopy under visible light and fluorescence.

were sacrificed, and the cecum was dissected. The cecum lesion scores were evaluated by the morphology of the intestinal contents, the thickness of the intestinal wall, and the degree of bleeding. The results showed that the cecum lesions in the G1 and G2 groups were lighter than those in the PC group (Fig. 7A), and the average cecum lesion score was 1.7, 1.4, and 2.7, respectively (Fig. 7B). Compared with the PC group, the reduction rate of cecal lesions in the G1 and G2 groups was 37.04% and 48.15%, respectively (Fig. 7C), with a significant difference ($p <$ 0.05). A comprehensive analysis of cecal lesion score and cecal lesion reduction rate revealed that the G2 group (morin treatment) could significantly improve cecal lesions compared with the PC group ($p <$ 0.05). Morin's improving effect on cecal lesions in *E. tenella*-infected chickens was generally dose-dependent.

3.9. Oocyst discharge

Feces of each group were collected 96–168 h after the coccidial attack and sampled after homogenization, and oocyst per gram feces (OPG) was counted with a McMaster slide. Morin could significantly reduce the oocyst production of *E. tenella*. Compared with the PC group, the oocyst discharge in morin-treated groups was significantly decreased ($p <$ 0.05). The oocyst reduction rate in the G1 and G2 groups was 35.15% and 32.88%, respectively, with no significant difference between the two groups (Fig. 7D).

3.10. Morin anticoccidial index

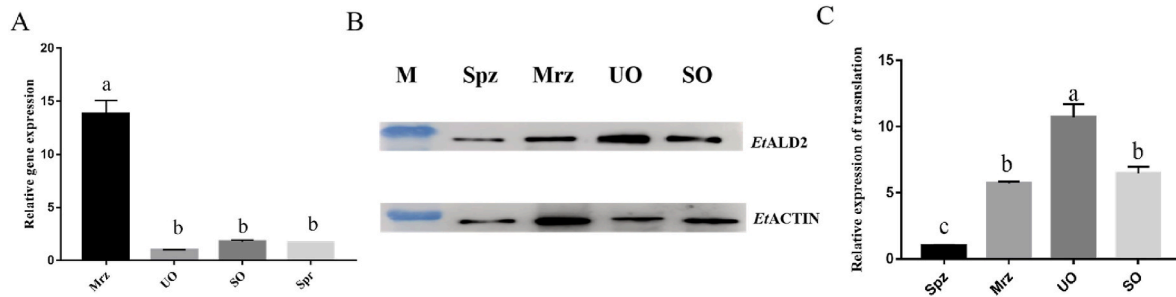Morin anticoccidial effect was dose dependent. The G1 group

Fig. 4. *Et*ALD2 mRNA (A) and protein (B, C) levels. Using *Et*18SrRNA as reference gene, $2^{-\Delta\Delta Ct}$ method was used to analyze the transcriptional levels of *Et*ALD2 in the four developmental stages of *E. tenella*. Using *Et*ACTIN as reference protein, mouse anti- *Et*ALD2 antibody was used to detect the protein levels at the four developmental stages. Mrz: second-generation merozoites; UO: unsporulated oocysts; SO: sporulated oocysts; Spr: sporozoites. Data are the mean and standard deviation of three independent experiments. Different letters in each group indicate significant differences ($p < 0.05$).
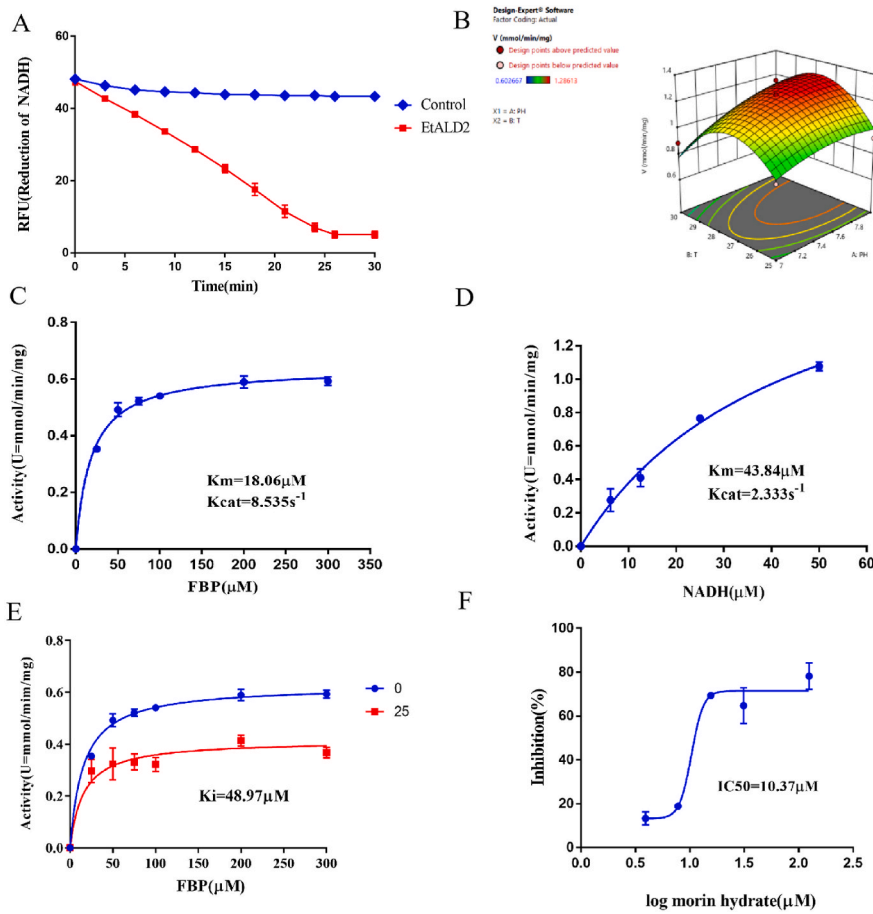

Fig. 5. *Et*ALD2 enzyme kinetics and *in vitro* inhibition constant of morin on *Et*ALD2. A. *Et*ALD2 catalyzed the reaction of fructose 1, 6-diphosphate, which was measured every 3 min and monitored continuously for 30 min. B. The optimum temperature and pH value of *Et*ALD2 were analyzed by RSM method. C-D. Variations in *Et*ALD2 activity at different substrate (fructose 1,6-bisphosphate and NADH) concentration. Means ± SD (n = 3). E. Michaelis-Menten-based analysis of the inhibition kinetics of morin (25 μM) on *Et*ALD2 as measured by NADH consumption. F. The effect of morin at increasing concentrations on the catalytic activity of *Et*ALD2. In the catalytic reaction, 4.03, 8.06, 16.12, 31.25, 62.50 and 125 μM morin were added to 100 μL reaction system. GraphPad Prism 7 was used to fit nonlinear regression curves and calculate IC$_{50}$ values.

Table 1
Effects of different substrates on the kinetic parameters of *Et*ALD2.

Parameter	FBP	NADH
K_m (μM)	18.06 ± 1.399	43.84 ± 6.587
$Vmax$ (mM·min^{-1})	0.64 ± 0.01	2.036 ± 0.175
$Kcat$ (S^{-1})	8.535	2.33
$Kcat/K_m$ (S^{-1}·M^{-1})	4.73×10^5	5.31×10^4

achieved a moderate anticoccidial effect, while the G2 group achieved a good anticoccidial effect. The anticoccidial indexes of the G1 and G2 morin administration groups were 149 and 162, respectively (Table 2), while the PC group had the lowest ACI (113).

4. Discussion

Aldolase is an attractive drug target for treating a variety of parasitic infections because of its enzymatic and non-enzymatic functions (Pirovich et al., 2021). In this study, we investigated the enzymatic function of *Et*ALD2. When we used NCBI to analyze the conserved domain of the *Et*ALD2 gene sequence, we found that *Et*ALD2 gene encodes a protein containing a conserved PTZ00019 domain. Further analysis showed that the gene belonged to the TIM superfamily.

To further study *Et*ALD2 protein function, we retrieved the homologous sequences of this gene in other parasite species from NCBI (https://www.ncbi.nlm.nih.gov/) and constructed the phylogenetic tree to explore the genetic relationship between ALD genes in different protozoan species. The results showed that the *Et*ALD2 gene was most
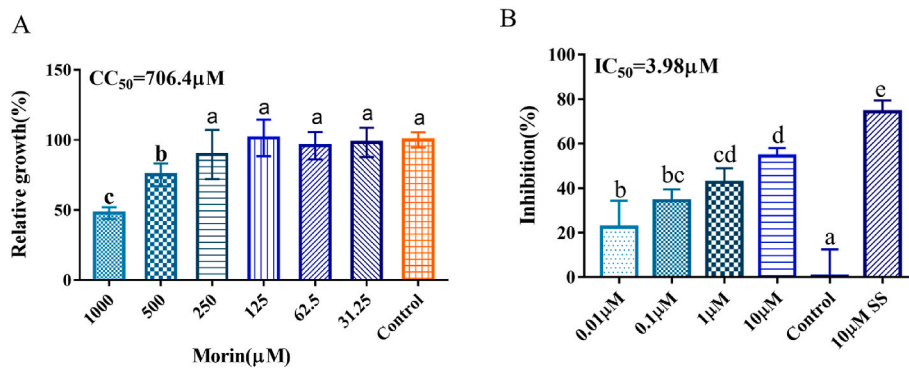
Fig. 6. Toxic effects of morin on MDBK cells (A) and inhibitory effect of morin on *E. tenella* development *in vitro* (B). In the cytotoxicity test, 0.5% DMSO was used as the negative control, and the absorbance was measured at 550 nm using a multifunctional microplate analyzer. The data were processed by GraphPad Prism7 software and CC_{50} values were calculated. All tests were repeated three times. In inhibitory test *in vitro*, 10 μM SS was used as a positive control. Different lowercase letters were used to indicate statistically significant differences ($p < 0.05$). The error bar represents mean ± SD (n = 3).
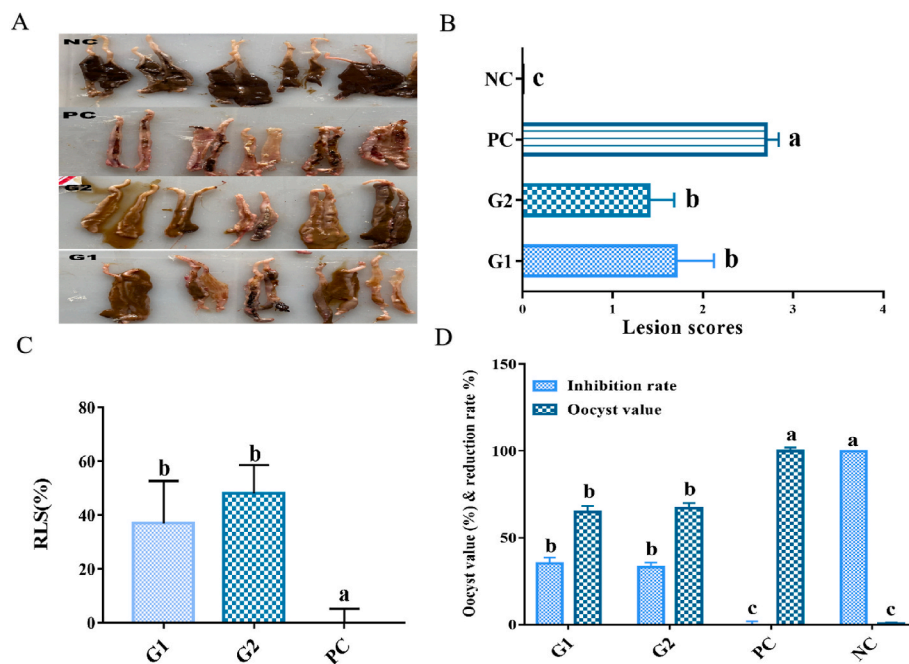

Fig. 7. Effects of morin on cecal lesions (A–C) and oocyst discharge (D) in chickens infected with *E. tenella*. Chickens were randomly divided into 4 groups with 10 chickens in each group. G1 and G2 were supplemented with 150 mg and 450 mg morin/Kg diet, respectively. PC and NC was infected nonmedicated and noninfected nonmedicated group. A : Cecum obtained on the 7th day after infection; B : Average cecal lesion score; C : Cecal lesions score reduction rate; D : Effects of morin on oocyst value and oocyst reduction rate. Different letters indicate significant differences among groups (p < 0.05) .

Table 2
Effects of morin on anticoccidial index of *E. tenella* infected chickens.

group	Relative weight gain rate (%)	Survival rate (%)	Lesion value	Oocyst value	ACI
Group 1	86.4	100	17	20	149
Group 2	95.9	100	14	20	162
Positive control	79.5	100	27	40	113
Negative control	100.0	100	0	0	200

closely related to ALD genes from *Cyclospora cayetanensis*, *Toxoplasma gondii*, and *Neospora caninum*. These protozoa are all apicomplexan species, suggesting that this gene is relatively conserved among apicomplexans. To verify this hypothesis, the five species (*Babesia bovis*, *Cyclospora cayetanensis*, *Neospora caninum*, *Plasmodium falciparum*, and *Toxoplasma gondii*) with the highest sequence homology to the *Et*ALD2 gene were compared. The *Et*ALD2 gene had high homology with the ALD domain of these other apicomplexan parasites, and the sequence was highly conserved. These data suggest that the function of *Et*ALD2 could be relatively conserved in different species, which may help *Et*ALD2 functional studies.

Eimeria tenella has a complex life cycle, including different developmental stages (El-Shall et al., 2022). Although *Et*ALD2 was transcribed and expressed in all four developmental stages, the *Et*ALD2 mRNA level in the second-generation merozoites was higher than that in sporozoites, sporulated oocysts, and unsporulated oocysts. However, many transcripts do not necessarily mean a corresponding number of translated proteins, which may be related to gene function at different stages of the parasite (Liang et al., 2021). This hypothesis may explain the higher protein level detected in unsporulated oocysts than in the second-generation merozoites. Generally, *Et*ALD2 protein was most highly expressed in the second-generation merozoites and unsporulated oocysts. These two developmental stages are the late endogenous stages of *E. tenella*, developing in the chicken intestinal tract and requiring high metabolic rates to obtain nutrients from host cells and escape the host immune response (Fetterer et al., 2007). The high *Et*ALD2 expression during development in host cells may be related to this protein's role in the glycolytic pathway, especially in second-generation merozoites. This finding suggests that *Et*ALD2 may be involved in the late endogenous development of the parasite, which may be an interesting topic for further study.

*Et*ALD2 was localized in the cytoplasm of *E. tenella* sporozoites, consistent with the localization in other apicomplexans (Shen and Sibley, 2014; Nemetski et al., 2015). Glycolysis occurs in the cytoplasm, and previous reports on aldolase localization also showed that aldolase was present in the cytoplasm, where it plays a conserved role in energy

metabolism. However, aldolases of some species, such as *Trichuris trichiura*, were not only localized in the cytoplasm but also on the cell membrane, where they perform many non-enzymatic functions (Pirovich et al., 2021).

We used the Michaelis-Menten model to fit the kinetic curve of the morin-mediated inhibition of *Et*ALD2. Morin was a non-competitive inhibitor of *Et*ALD2 and could reversibly bind to the enzyme-substrate complex and the enzyme itself. Non-competitive inhibition is more favorable than competitive inhibition in drug development because high substrate concentrations cannot reverse inhibition (Hartuti et al., 2018).

In vitro inhibition experiments demonstrated that morin could inhibit the development of *E. tenella* with an IC$_{50}$ value of 3.98 μM. Studies have shown that plant-derived phenolic compounds (including flavonoids and phenolic acids) have an inhibitory effect on coccidia, and phenolic hydroxyl groups may greatly contribute to this anticoccidial activity (El-Saadony et al., 2021; El-Shall et al., 2022). *In vivo* experiment results revealed that the addition of morin at a 450 mg/kg feed dose could achieve a good anticoccidial effect, and the SI value was 177.49, with a high safety factor. Additionally, morin feed supplement significantly decreased oocyst discharge and improved cecal lesions of *E. tenella*-infected chickens. Recently, scholars have devoted themselves to seeking "green" anticoccidial drugs from natural product extracts (Quiroz-Castañeda and Dantán-González, 2015). As a common natural compound in Chinese herbal medicine and dietary supplements, the safety of morin has been thoroughly studied and confirmed, achieving satisfactory results (Jiang et al., 2020; Khamchai et al., 2020). A recent study has shown that morin, as a feed additive, had the potential to protect poultry liver and kidneys, prevent harmful substances in feed, and improve poultry production performance (Gao et al., 2021). Together, these results indicate that morin has a good application prospect for coccidiosis control.

In the structure of morin, phenolic hydroxyl groups are present at the C3 position, A ring 5,7 position and B ring 2,4 position of the flavonoid skeleton. Similarly, there are phenolic hydroxyl groups in quercetin at the C3 position, A ring 5,7 position and B ring 3,4 position of the flavonoid skeleton; in kaempferol at the C3 position, A ring 5,7 position and B ring 4 position of the flavonoid skeleton; and in fisetin at the C3 position, A ring 7 position and B ring 3,4 position of the flavonoid skeleton. All three flavonoids, quercetin, kaempferol, and fisetin, showed strong antiparasitic activity (Panda and Luyten, 2018). Furthermore, Quintanilla-Licea et al. (2020) analyzed the antiparasitic activity of different flavonoids with similar structures. They displayed that adding phenolic hydroxyl at position 7 of the A ring significantly improved antiparasitic activity. However, after adding a phenolic hydroxyl group to position 4 of the B ring, there was little difference in antiprotozoal activity. Notably, phenolic hydroxyl groups in glabridin showed strong antiparasitic activity only at positions 2 and 4 of the B ring of the flavonoid skeleton (Cheema et al., 2014). These results suggest that the phenolic hydroxyl groups at position 7 of the A ring and position 2 of the B ring in the flavonoid skeleton may significantly contribute to the antiparasitic activity.

5. Conclusion

*Et*ALD2 was localized in the cytoplasm of *E. tenella* sporozoites and plays a conserved role in energy metabolism. *Et*ALD2 mRNA and protein were highly expressed in the late stage of infection, suggesting that *Et*ALD2 may be involved in the late stages of the parasite endogenous development. Morin significantly improved cecal lesions of *E. tenella* infected chickens and reduced oocyst excretion. The anticoccidial index of the morin-treated group (450 mg/kg feed) was 162, indicating a good anticoccidial effect. Morin showed strong anticoccidial activity, which may be due to the interaction of the phenolic hydroxyl group at position 7 of the A ring and position 2 of the B ring of its flavonoid skeleton with *Et*ALD2 active site.

References

Blake, D.P., Knox, J., Dehaeck, B., Huntington, B., Rathinam, T., Ravipati, V., Ayoade, S., Gilbert, W., Adebambo, A.O., Jatau, I.D., Raman, M., Parker, D., Rushton, J., Tomley, F.M., 2020. Re-calculating the cost of coccidiosis in chickens. Vet. Res. 51, 1–14.

Bu, P., Chen, K., Xiang, K., Johnson, C., Crown, S.B., Rakhilin, N., Ai, Y., Wang, L., Xi, R., Astapova, I., Han, Y., Li, J., Barth, B.B., Lu, M., Gao, Z., Mines, R., Zhang, L., Herman, M., Hsu, D., Zhang, G., Shen, X., 2018. Aldolase B-mediated fructose metabolism drives metabolic reprogramming of colon cancer liver metastasis. Cell Metabol. 27, 1249–1262.

Cáceres, A.J., Michels, P.A.M., Hannaert, V., 2010. Genetic validation of aldolase and glyceraldehyde-3-phosphate dehydrogenase as drug targets in *Trypanosoma brucei*. Mol. Biochem. Parasitol. 169, 50–54.

Cai, X., Fuller, A.L., McDougald, L.R., Zhu, G., 2003. Apicoplast genome of the coccidian *Eimeria tenella*. Gene 321, 39–46.

Cheema, H.S., Prakash, O., Pal, A., Khan, F., Bawankule, D.U., Darokar, M.P., 2014. Glabridin induces oxidative stress mediated apoptosis like cell death of malaria parasite *Plasmodium falciparum*. Parasitol. Int. 63, 349–358.

Dax, C., Duffieux, F., Chabot, N., Coincon, M., Sygusch, J., Michels, P.A.M., Blonski, C., 2006. Selective irreversible inhibition of fructose 1,6-bisphosphate aldolase from *Trypanosoma brucei*. J. Med. Chem. 49, 1499–1502.

Edgar, R.C., Sjolander, K., 2004. A comparison of scoring functions for protein sequence profile alignment. Bioinformatics 20, 1301–1308.

El-Saadony, M.T., Zabermawi, N.M., Zabermawi, N.M., Burollus, M.A., Shafi, M.E., Alagawany, M., Yehia, N., Askar, A.M., Alsafy, S.A., Noreldin, A.E., Khafaga, A.F., Dhama, K., Elnesr, S.S., Elwan, H.A.M., Cerbo, A.D., El-Tarabily, K.A., Abd El-Hack, M.E., 2021. Nutritional aspects and health benefits of bioactive plant compounds against infectious diseases: a review. Food Rev. Int. 1–23.

El-Shall, N.A., Abd El-Hack, M.E., Albaqami, N.M., Khafaga, A.F., Taha, A.E., Swelum, A. A., El-Saadony, M.T., Salem, H.M., El-Tahan, A.M., AbuQamar, S.F., El-Tarabily, K. A., Elbestawy, A.R., 2022. Phytochemical control of poultry coccidiosis: a review. Poultry Sci. 101, 101542.

Fetterer, R.H., Miska, K.B., Lillehoj, H., Barfield, R.C., 2007. Serine protease activity in developmental stages of *Eimeria tenella*. J. Parasitol. 93, 333–340.

Gao, X., Xu, J., Jiang, L., Liu, W., Hong, H., Qian, Y., Li, S., Huang, W., Zhao, H., Yang, Z., Liu, Q., Wei, Z., 2021. Morin alleviates aflatoxin B1-induced liver and kidney injury by inhibiting heterophil extracellular traps release, oxidative stress and inflammatory responses in chicks. Poultry Sci. 100, 101513.

Han, H.Y., Lin, J.J., Zhao, Q.P., Dong, H., Jiang, L.L., Xu, M.Q., Zhu, S.H., Huang, B., 2010. Identification of differentially expressed genes in early stages of *Eimeria tenella* by suppression subtractive hybridization and cDNA microarray. J. Parasitol. 96, 95–102.

Hartuti, E.D., Inaoka, D.K., Komatsuya, K., Miyazaki, Y., Miller, R.J., Xinying, W., Sadikin, M., Prabandari, E.E., Waluyo, D., Kuroda, M., Amalia, E., Matsuo, Y., Nugroho, N.B., Saimoto, H., Pramisandi, A., Watanabe, M., Mori, M., Shiomi, K., Balogun, E.O., Shiba, T., Harada, S., Nozaki, T., Kita, K., 2018. Biochemical studies of membrane bound *Plasmodium falciparum* mitochondrial L-malate:quinone oxidoreductase, a potential drug target. Biochim. Biophys. Acta Bioenerg. 1859, 191–200.

Jiang, A., Zhang, Y., Zhang, X., Wu, D., Liu, Z., Li, S., Liu, X., Han, Z., Wang, C., Wang, J., Wei, Z., Guo, C., Yang, Z., 2020. Morin alleviates LPS-induced mastitis by inhibiting the PI3K/AKT, MAPK, NF-κB and NLRP3 signaling pathway and protecting the integrity of blood-milk barrier. Int. Immunopharm. 78, 105972.

Jin, Z., Ma, J., Zhu, G., Zhang, H., 2019. Discovery of novel anti-cryptosporidial activities from natural products by *in vitro* high-throughput phenotypic screening. Front. Microbiol. 1999. .

Khamchai, S., Chumboatong, W., Hata, J., Tocharus, C., Suksamrarn, A., Tocharus, J., 2020. Morin protects the blood–brain barrier integrity against cerebral ischemia reperfusion through anti-inflammatory actions in rats. Sci. Rep. 10, 1–13. .

Kumar, S., Stecher, G., Tamura, K., 2016. MEGA7: molecular evolutionary genetics analysis version 7.0 for bigger datasets. Mol. Biol. Evol. 33, 1870–1874.

Lee, Y., Lu, M., Lillehoj, H.S., 2022. Coccidiosis: recent progress in host immunity and alternatives to antibiotic strategies. Vaccines 10, 215.

Li, G., Wang, G., Li, M., Li, L., Liu, H., Sun, M., Wen, Z., 2020. Morin inhibits *Listeria monocytogenes* virulence *in vivo* and *in vitro* by targeting listeriolysin O and inflammation. BMC Microbiol. 20, 1–9.

Liang, S., Dong, H., Zhu, S., Zhao, Q., Huang, B., Yu, Y., Wang, Q., Wang, H., Yu, S., Han, H., 2021. *Eimeria tenella* translation initiation factor eIF-5A that interacts with calcium-dependent protein kinase 4 is involved in host cell invasion. Front. Cell. Infect. Microbiol. 870.

Liu, Q., Jiang, Y., Yang, W., Liu, Y., Shi, C., Liu, J., Gao, X., Huang, H., Niu, T., Yang, G., Wang, C., 2020. Protective effects of a food-grade recombinant *Lactobacillus plantarum* with surface displayed AMA1 and *Et*MIC2 proteins of *Eimeria tenella* in broiler chickens. Microb. Cell Factories 19, 1–18.

Marugan-Hernandez, V., Jeremiah, G., Aguiar-Martins, K., Burrell, A., Vaughan, S., Xia, D., Randle, N., Tomley, F., 2020. The growth of *Eimeria tenella*: characterization and application of quantitative methods to assess sporozoite invasion and endogenous development in cell culture. Front. Cell. Infect. Microbiol. 568.

Nemetski, S.M., Cardozo, T.J., Bosch, G., Weltzer, R., O Malley, K., Ejigiri, I., Kumar, K. A., Buscaglia, C.A., Nussenzweig, V., Sinnis, P., Levitskaya, J., Bosch, J., 2015. Inhibition by stabilization: targeting the *Plasmodium falciparum* aldolase–TRAP complex. Malar. J. 14, 1–18.

Panda, S.K., Luyten, W., 2018. Antiparasitic activity in Asteraceae with special attention to ethnobotanical use by the tribes of Odisha, India. Parasite 25, 10.

Pirovich, D.B., Da Dara, A.A., Skelly, P.J., 2021. Multifunctional fructose 1,6-bisphosphate aldolase as a therapeutic target. Front. Mol. Biosci. 8.

Qaid, M.M., Al-Mufarrej, S.I., Azzam, M.M., Al-Garadi, M.A., 2021. Anticoccidial effectivity of a traditional medicinal plant, *Cinnamomum verum*, in broiler chickens infected with *Eimeria tenella*. Poultry Sci. 100, 100902.

Quintanilla-Licea, R., Vargas-Villarreal, J., Verde-Star, M.J., Rivas-Galindo, V.M., Torres-Hernández, Á.D., 2020. Antiprotozoal activity against *Entamoeba histolytica* of flavonoids isolated from lippia graveolens kunth. Molecules 25, 2464.

Quiroz-Castañeda, R.E., Dantán-González, E., 2015. Control of avian coccidiosis: future and present natural alternatives. BioMed Res. Int. 2015.

Shen, B., Sibley, L.D., 2014. *Toxoplasma* aldolase is required for metabolism but dispensable for host-cell invasion. Proc. Natl. Acad. Sci. USA 111, 3567–3572.

Sun, M., Liao, S., Zhang, L., Wu, C., Qi, N., Lv, M., Li, J., Lin, X., Zhang, J., Xie, M., Zhu, G., Cai, J., 2016. Molecular and biochemical characterization of *Eimeria tenella* hexokinase. Parasitol. Res. 115, 3425–3433.

Thabet, A., Zhang, R., Alnassan, A., Daugschies, A., Bangoura, B., 2017. Anticoccidial efficacy testing: *In vitro Eimeria tenella* assays as replacement for animal experiments. Vet. Parasitol. 233, 86–96.

Wei, Z., He, X., Kou, J., Wang, J., Chen, L., Yao, M., Zhou, E., Fu, Y., Guo, C., Yang, Z., 2015. Renoprotective mechanisms of morin in cisplatin-induced kidney injury. Int. Immunopharm. 28, 500–506.

Yang, Y., Bai, X., Li, C., Tong, M., Zhang, P., Cai, W., Liu, X., Liu, M., 2019. Molecular characterization of fructose-1,6-bisphosphate aldolase from *Trichinella spiralis* and its potential in inducing immune protection. Front. Cell. Infect. Microbiol. 9, 1–11.

Zhang, J.J., Wang, L.X., Ruan, W.K., An, J., 2013. Investigation into the prevalence of coccidiosis and maduramycin drug resistance in chickens in China. Vet. Parasitol. 191, 29–34.

Zhang, Y., Zuo, R., Song, X., Gong, J., Wang, J., Lin, M., Yang, F., Cheng, X., Gao, X., Peng, L., Ji, H., Chen, X., Jiang, S., Guo, D., 2022. Optimization of maduramicin ammonium-loaded nanostructured lipid carriers using box–behnken design for enhanced anticoccidial effect against *Eimeria tenella* in broiler chickens. Pharmaceutics 14, 1330.

Zhou, B.H., Wang, H.W., Wang, X.Y., Zhang, L.F., Zhang, K.Y., Xue, F.Q., 2010. *Eimeria tenella*: effects of diclazuril treatment on microneme genes expression in second-generation merozoites and pathological changes of caeca in parasitized chickens. Exp. Parasitol. 125, 264–270.